First-Principle Electronic Properties of Dilute-As GaNAs Alloy for Visible Light Emitters

Chee-Keong Tan, Jing Zhang, Xiao-Hang Li, Guangyu Liu, Benjamin O. Tayo, and Nelson Tansu

***Abstract*—The band structure of dilute-As GaNAs alloy with the As composition range from 0% to 12.5% is studied by using First-Principle density-functional calculation. Our analysis shows that the dilute-As GaNAs alloy exhibits the direct band gap properties. The dilute-As GaNAs alloy shows a band gap range from 3.645 eV down to 2.232 eV with As content varying from 0% to 12.5%, which covers the blue and green spectral regime. This finding indicates the alloy as a potential candidate for photonic devices applications. The bowing parameter of 14.5 eV $\pm$ 0.5 eV is also obtained using line fitting with the First-Principle and experimental data. The effective masses for electrons and holes in dilute-As GaNAs alloy, as well as the split-off energy parameters, were also presented. Minimal interband Auger recombination is also suggested for the dilute-As GaNAs alloy attributing to the off-resonance condition for this process.**

***Index Terms*—Auger recombination, band parameters, band structure, dilute-As GaNAs, First-Principle, lasers, light-emitting diodes.**

I. Introduction

GROUP III-Nitride semiconductor presents as a vital semiconductor group for visible emitters and energy efficiency technologies [1]–[9]. More importantly, the III-Nitride semiconductor possesses many desirable electronics and optoelectronic properties, notably its direct and large band gap in the Brillouin Zone (BZ). A prime example of such semiconductor is the AlGaInN alloy acquiring the energy band gap varying from 0.7 eV up to 6.2 eV, which covers the entire visible spectral regime, as well as the ultraviolet and the infrared spectrum. Therefore, this III-Nitride compound plays a critical role in the optoelectronic applications such as light-emitting diodes (LEDs) and laser diodes.

The rapid development of InGaN, AlGaN and AlInN alloys in the past decade are primarily driven by the strong need for addressing high-efficiency green- and blue-emitting LEDs [4]. In contrast to the InGaN and AlGaN alloys, the progress in dilute-As GaNAs compound semiconductor is relatively at its early stage. There are significant studies and advances in the field of dilute-N (In)GaAsN-based alloy, leading to the state-of-the-art and low threshold laser devices for telecommunication applications [10]–[12]. These advances were driven by the progress in material epitaxy, improved device physics understanding, and improved understanding of the electronic band structure of the dilute-N GaNAs alloy [10]–[14]. Nonetheless, with regards to the theoretical and experimental study of dilute-As GaNAs alloy, the literature available through the published manuscripts is severely limited [5], [15]–[23]. In other words, the pursuit of dilute-As GaNAs alloy is still at its infancy.

The arsenic impurity was first successfully incorporated by Li and co-workers into the thin film GaN through metal-organic chemical vapor deposition (MOCVD) [5]. Building on the first successful synthesis of dilute-As GaNAs alloy by Li and co-workers [5], Kimura and co-workers reported the growths of dilute-As GaNAs alloy with As-content up to 6.7% As-content with MOCVD [15]. Most recently, Yu and co-workers reported the synthesis of dilute-As GaNAs alloy by using non-equilibrium low temperature molecular beam epitaxy method [16]. Both works have demonstrated that the band gap of GaNAs alloy reduces, as As-content is incorporated into the alloy. The band gap reduction in dilute-As GaNAs alloy enables the wavelength coverage in the entire visible spectrum [15]–[17], which shows good potential for this alloy as alternative novel semiconductor material for the visible light applications. Hence, the understanding of the electronic properties and band parameters of dilute-As GaNAs alloy is of great importance for further development of this alloy for the laser and light emitting diode applications.

Due to the technological importance that is potentially inflicted by dilute-As GaNAs alloy, accurate prediction of the electronic properties and the optical properties on the alloy is highly desirable. A lack of experimental data and electronic structure information on the GaNAs alloy hereinafter requires theoretical study that utilizes experiment-parameter-free calculation specifically Density Functional Theory (DFT) on the alloy. The DFT study will harness the insightful information regarding to the band parameters, which will be useful for device physics and simulation in development of dilute-As GaNAs semiconductor optoelectronics devices.

In this work, we present the analysis of the electronic properties of dilute-As GaNAs by using First-Principle Density Functional Theory. The Arsenic (As) atoms with different As concentrations varying from 0% up to 12.5% are introduced into the GaN material as impurities in the alloy. The band structure, energy band gap, and electronic properties of the dilute-As GaNAs alloy are presented. In addition, the resonance energy condition

Manuscript received January 17, 2013; accepted February 19, 2013. Date of publication March 07, 2013; date of current version March 15, 2013. This work was supported by the U.S. National Science Foundation under Grant ECCS-1028490 and Grant DMR-0907260 and by the Class of 1961 Professorship Fund.

The authors are with the Center for Photonics and Nanoelectronics, Department of Electrical and Computer Engineering, Lehigh University, Bethlehem, PA 18015 USA (e-mail: ckt209@lehigh.edu; tansu@lehigh.edu).

Color versions of one or more of the figures are available online at http://ieeexplore.ieee.org.

Digital Object Identifier 10.1109/JDT.2013.2248342

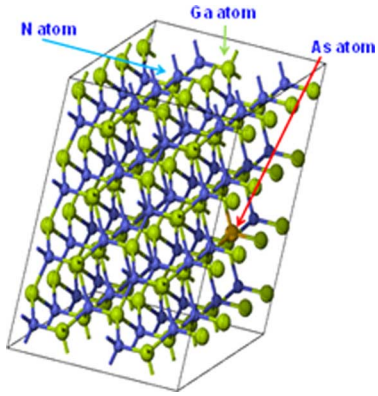

Fig. 1. A 4×4×2 supercell is built using MedeA-VASP software. This 128-atom supercell consists of 64 Gallium (Ga) atoms, 63 Nitrogen (N) atoms and 1 Arsenic (As) atom, corresponding to 1.56% As-content in GaNAs.

of the alloy is analyzed, and its effect on the interband Auger recombination rate is also briefly discussed. The DFT results for the dilute-As GaNAs alloy show good agreement with the experimental data.

II. Computational Method

In our DFT analysis, the supercell approach was used to build appropriate crystal structures for the band calculations. To illustrate the supercell approach, Fig. 1 shows a constructed GaNAs alloy crystal structure with 4×4×2 supercell consisting of a total of 128 atoms. The 128-atom model of GaNAs crystal consists of 64 Ga atoms, 63 N atoms and 1 substituted As atom, corresponding to 1.56% As in the dilute-As alloy. The band structure calculations were performed by using the projector augmented wave (PAW) method as implemented in the MedeA-VASP software [24]. The use of local density approximation (LDA) exchange-correlation potential was employed in the calculation. The electronic wave functions are described in plane wave basis with a cutoff energy of 400 eV. The structure optimization was performed by relaxing the atom positions with the Hellmann-Feynman force set to 0.02 eV/Å. The external stress was set to 0 GPa, and the energy convergence tolerance was set to 1×10^{-5} eV/atom. The Gamma-centered Monkhorst-Pack grid and high symmetry k-points were used for the band structure calculations. Note that different Monkhorst-Pack k-point meshes were generated in the calculations attributed to the use of different supercell sizes. The spin-orbit coupling was excluded in the calculation, as its effect in the wide band gap III-nitride semiconductor is insignificant.

III. Band Structures and Parameters of Dilute-As GaNAs Alloy

Fig. 2(a) and (b) show the band structures for GaN and $GaN_{0.9375}As_{0.0625}$ (6.25% As-content) alloys calculated by using the DFT method respectively. From our analysis, the conduction band minimum (CBM) and valence band maximum (VBM) for dilute As-content GaNAs (up to 12.5% As-content) exhibited direct band gap properties, indicating its suitability for photonics device applications. The energy band gaps for dilute-As GaNAs alloy were obtained from the difference between the CBM and the VBM taking into account the scissor

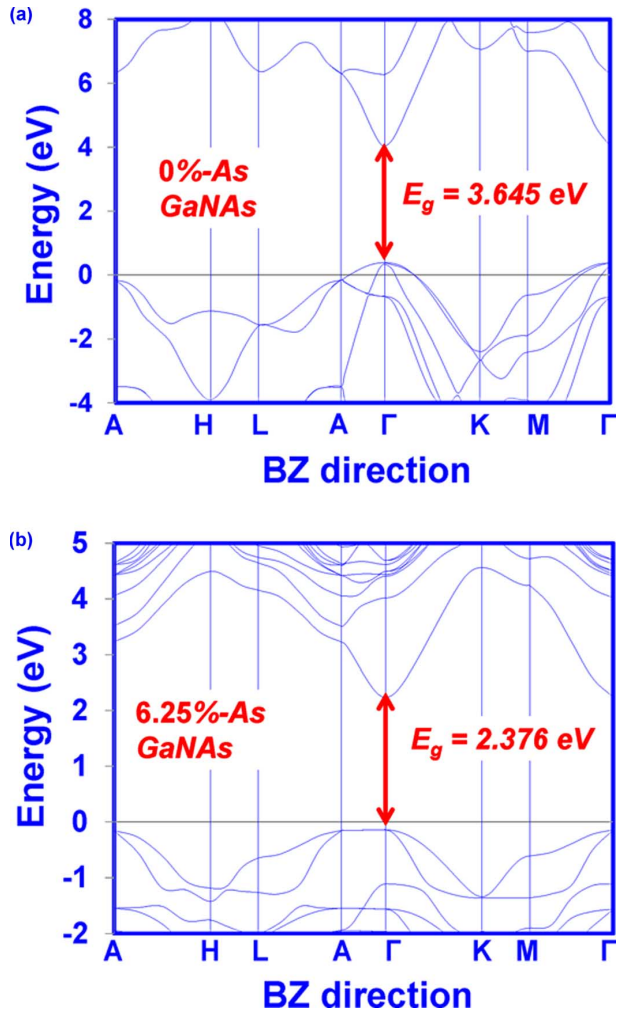

Fig. 2. Band structure diagrams for GaNAs alloy with (a) 0% and (b) 6.25% As-content. Energy band gap is the energy difference between the conduction band minimum (CBM) and valence band maximum (VBM).

operator [25]. The scissor operator was employed to correct the band gap error originated from the LDA calculation [25]. From the above figures, it is shown that the incorporation of tiny amount of Arsenic impurity into the GaN alloy could lead to the significant reduction in the band gap energy of the alloy. Based on the initial finding, further investigation on the dilute-As GaNAs alloy was carried out in order to gain more information on the alloy.

Fig. 3(a) shows the comparison of the DFT-calculated and experimental energy band gaps for dilute-As GaNAs alloy as a function of As-content in the alloy. Kimura and co-workers reported the experimental data for energy band gaps measured from MOCVD-grown dilute-As GaNAs alloy [15], and the numerical results show good agreement with these experimental data. Fig. 3(a) shows that when the As-content in the GaNAs alloy increases, the energy band gap of the alloy reduces. The energy band gap covers from 3.645 eV to 2.232 eV for the GaNAs alloy with As-content up to 12.5%.

Slight discrepancies between the calculated and the measured results were observed, however the trend shows reduction in bandgap as the As-content increases in the dilute-As GaNAs alloy. While these discrepancies potentially arise from the strain

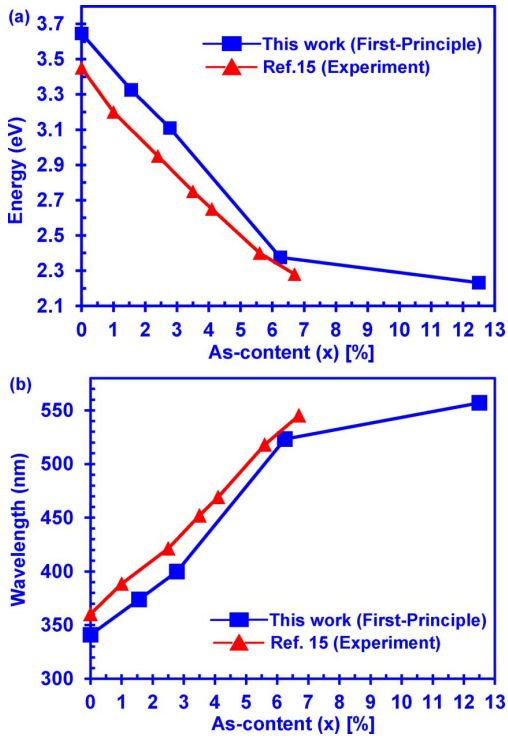

Fig. 3. (a) Energy band gap and (b) emission wavelength of dilute-As GaNAs alloy from As-content of 0% up to 12.5%, ranging from 3.645 eV down to 2.232 eV, with corresponding experimental data [15].

effect in the alloy and/or As-clustering effect in the GaNAs alloy grown by MOCVD, another reason is that the band gap information was obtained at two temperature conditions. Our calculation was set for zero-temperature limit, which is commonly used in DFT calculation [26], [27]. The optical absorption and reflection measurements by Kimura and co-workers were performed at room temperature. As stated by Shishkin and co-workers [27], the experimental temperature dependence for the band gap of material is significant and highly dependent on material quality, thus the band gaps of materials will be more accurate for comparison at low temperature whenever possible. However, the available experimental data on dilute-As GaNAs was limited to room-temperature results [15], [23], thus restricting the possibility for comparison at similar temperature. Furthermore, as stated in Section II, the band gap problem is well known in DFT calculation. All these conditions would lead to the discrepancies of the result in comparison.

Since the temperature-dependent band gap of semiconductors is known to reduce when the temperature increases [28]–[30], one could perform molecular dynamics simulation for thermal expansion, with the expense of the computational cost. The Varshni relation [29], [30] can be used for including the temperature dependence of energy band gap. However, it is to be emphasized that this work is aimed to provide the necessary band parameter information of dilute-As GaNAs alloy, as well as its potential application for LEDs/lasers in the visible spectral regimes.

On the other hand, the effect of As impurity in lowering down the energy band gap of dilute-As GaNAs alloy can be attributed primarily to the upward movement of the valence

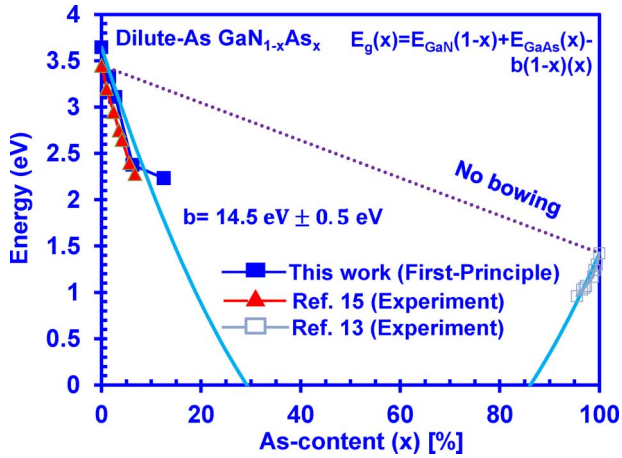

Fig. 4. Comparison between our DFT calculations and experimental data, with bowing parameter obtained through line fitting with the data.

band of the alloy after the As impurity incorporation into the alloy [16], [23]. Moreover, it is also expected to observe similar effect should the As impurity be incorporated into InGaN ternary alloy, resulting in the reduction of energy band gap of the ternary alloy. Nevertheless, this work is focused in the electronic structure of dilute-As GaNAs alloy and its potential use as the optoelectronic devices. Further study on the effect of As impurity on InGaN ternary alloy would be necessary in order to gauge its usefulness for the visible light emitters.

Fig. 3(b) shows the emission wavelength as a function of As-content in the dilute-As GaNAs alloy. It is shown that the light emission wavelength is in the region of 400 nm with As-content of 2.78% in the dilute-As GaNAs alloy which can be used for violet LEDs applications. In addition, the light emission wavelength reaches 523 nm with As-content of 6.25% in the GaNAs alloy. This suggests the possibility of the alloy to be implemented as active region for green-emitting LEDs. Further incorporation of As-content up to 12.5% in the GaN alloy leads to the 560 nm light emission wavelength, hinting the possibility of yellow/red light emission should more As-content be incorporated into the dilute-As GaNAs alloy. Note that the existence of polarization field in the III-Nitride active region will also lead to the conduction and valence bands bending [3], [21], [23], which in turn results in red shift of the emission wavelengths [3], [21], [23]. Thus, yellow or red light emission might be achieved with low As-content in dilute-As GaNAs QW under the polarization effect.

Fig. 4 displays the energy band gap of GaNAs alloy in the whole composition range. The dotted line in Fig. 4 represents the band gap result by using the virtual crystal approximation (VCA). The overall composition dependence of the alloy band gap is written as $\mathrm{E_g}(x) = \mathrm{E_{GaN}}(1\text{-}x) + \mathrm{E_{GaAs}}(x)$. This VCA linear interpolation indicates the important effects of the molar fraction of the GaAs or GaN component in the alloy onto the band gap changes. The VCA result without bowing parameter is largely different from the calculated and the experimental data. The linear Vegard relation is thus extended by adding the bowing parameter into the expression. The solid line in the figure shows a line fitting with the DFT-calculated data and the experimental data through the use of the following equation

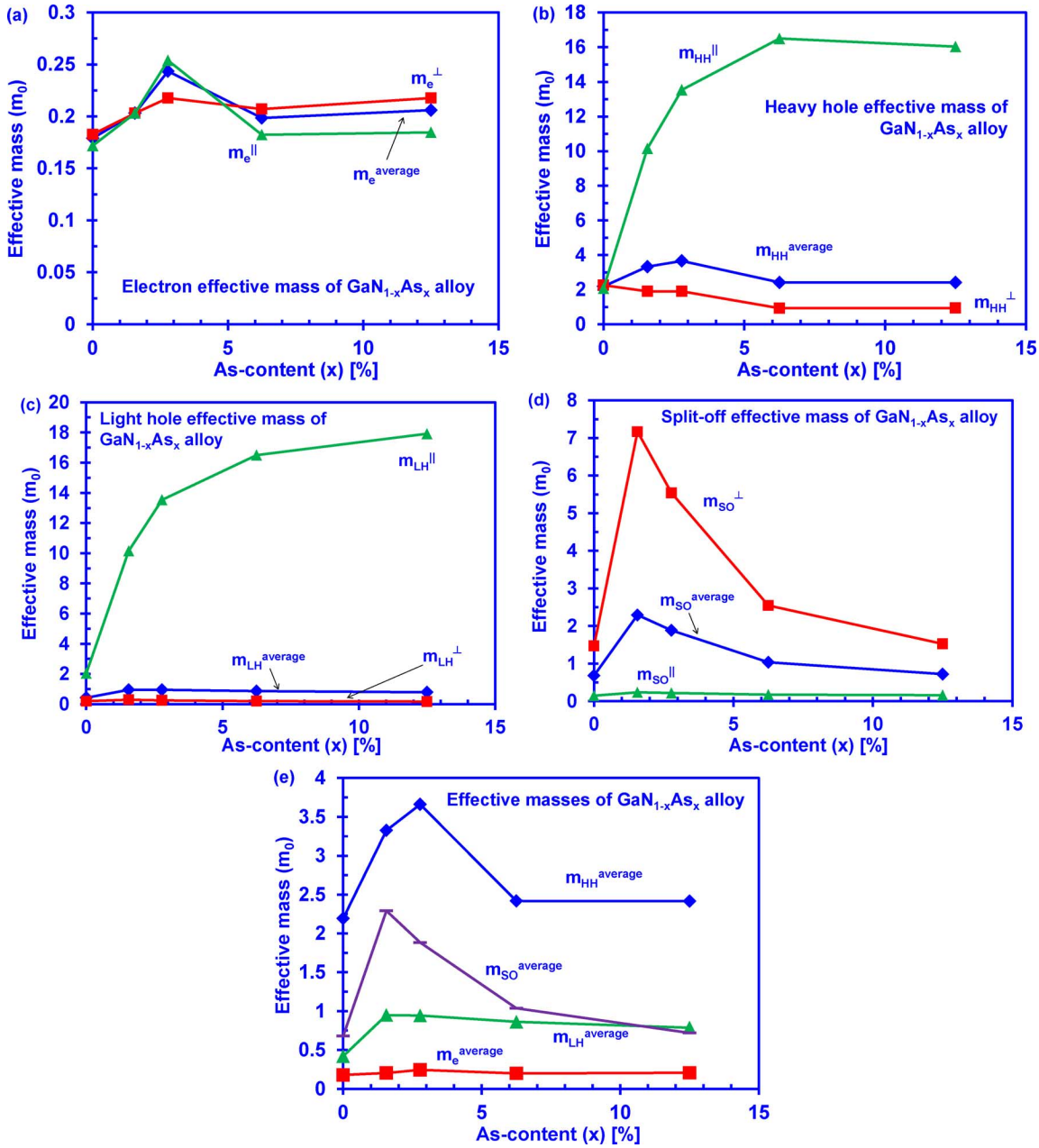

Fig. 5. Carrier effective masses obtained through energy dispersion relation and parabolic line fitting with the calculated DFT band for: (a) electron; (b) heavy hole; (c) light hole; (d) split-off bands; and (e) comparison of average carrier effective masses as a function of As-content in GaNAs alloy.

$\mathrm{E_g}(x) = \mathrm{E_{GaN}}(1\text{-}x) + \mathrm{E_{GaAs}}(x) - \mathrm{b}(1\text{-}x)(x)$. The bowing parameter of $\mathrm{b} = 14.5\ \mathrm{eV} \pm 0.5\ \mathrm{eV}$ is found to have a reasonable matching with the energy band gap data. Meanwhile, bowing parameter in the 16 eV range were suggested previously [15], [16], but it appears that the line fit does not agree very well with our data. Along this quadratic curve, the band gap would rapidly reduce from both ends and become negative within 25% to 85% of As-content of the alloy. This can be understood through the formulated Hamiltonian matrices in the degenerate perturbation theory, explaining that the composition dependency on the N-rich side is more than just a simple quadratic function [23].

Fig. 5 present the carrier effective masses of the dilute-As GaNAs alloy. The parabolic line fitting method is used in obtaining the effective mass parameter [31]. A parabolic line fit to the conduction band dispersion relation is used to determine the effective mass of electrons. For GaN alloy, the $\mathrm{m_e} = 0.2\mathrm{m_o}$ in the $\mathrm{k_z}$ direction and $\mathrm{m_e} = 0.17\mathrm{m_o}$ in the $\mathrm{k_x k_y}$ direction. The parabolic line fitting method is also used for the valence bands consisting of heavy hole, light hole and split-off bands. The effective mass parameters are obtained along the $\mathrm{k_z}$ direction, as well as the in plane direction ($\mathrm{k_x k_y}$) near the gamma point. The average effective mass is also obtained for the electrons, heavy hole, light hole and split-off. It is shown in the Fig. 5 that the electron effective mass only varies slightly from 0% As-content to 12.5% As-content. Interestingly, the hole effective mass changes rapidly from 0% to 6.25% As-content, but remains constant in a higher percentage of As-content in the GaNAs alloy.

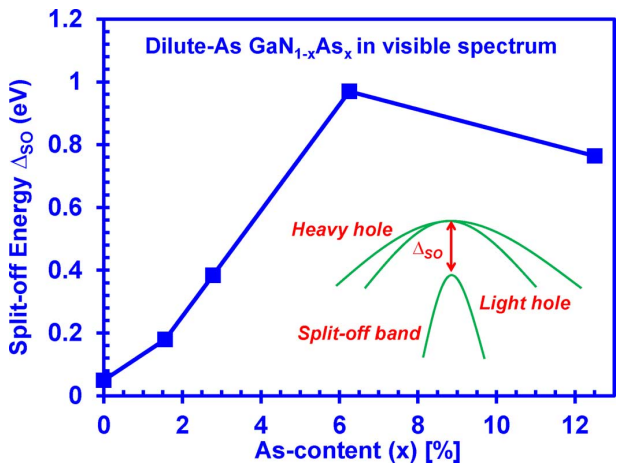

Fig. 6. Split-off energy of dilute-As GaNAs alloy from 0% up to 12.5% As-content, obtained through the energy difference between the valence band maximum (VBM) and the split-off band (SO) at Γ-point in Brillouin Zone.

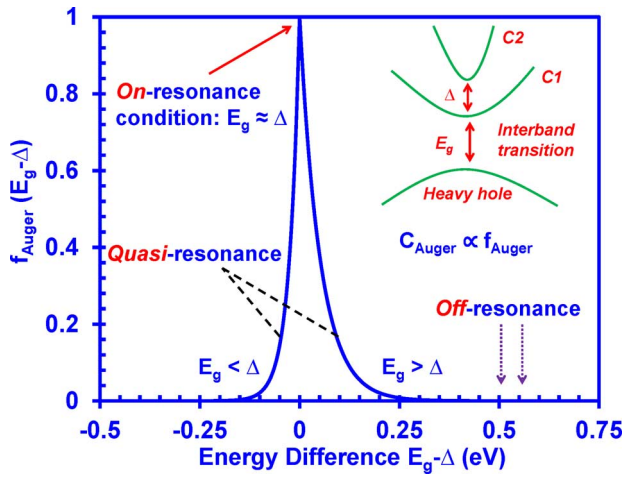

Fig. 7. Interband Auger function (f_{Auger}) as a function for energy difference E_g-Δ of dilute-As GaNAs alloy. The f_{Auger} is proportional to the Auger recombination coefficient, resulting in the increased coefficient under resonance condition.

From Fig. 5(e), our analysis shows that the electron effective masses for dilute-As GaNAs alloy are relatively unchanged for all compositions studied here, which are very different than the corresponding characteristics observed in dilute-nitride based (In)GaAsN alloy [14]. For dilute-nitride based (In)GaAsN alloy, the electron effective mass have remarkable changes, while the effective masses for hole bands remained unchanged. The reason behind this is that the addition of nitrogen atoms into the dilute-nitride GaAsN alloy plays a key role in the modification of conduction band structure, due to its strong localized resonant energy level close to the conduction band. In contrast, the incorporation of As atoms into the dilute-As GaNAs alloy leads to significant modification in the effective masses for the heavy hole in the material, while the electron effective masses remain largely unperturbed by the impurity addition. Consequently, the possible explanation of the effect shown in the effective masses can be attributed to the impurity level of As-localized states in the bands. The localized As states was theoretically predicted to possess an energy level of 0.4 eV above the uppermost valence band [23], which leads to strong modification of the hole bands in dilute-As GaNAs alloy.

Fig. 6 shows the split-off energy of dilute-As GaNAs alloy as a function of As-content. The introduction of As-content in the GaNAs alloy results in the general increase of split-off energy. This characteristic is interesting in the fact that both GaN and GaAs alloys possess split-off energy less than 0.5 eV [32] while the dilute-As GaNAs alloy has significant increase of split-off energy at low As-content.

Based on our finding, for higher As-content dilute-As ($>6.25\%$) GaNAs alloy, the As clustering effect appears to play significant role resulting in deviation from the trend exhibited in the band parameters for the lower As-content dilute-As GaNAs alloy. In addition, the structural changes had also been reported for high As-content GaNAs alloy [16], which may lead to any deviation. Further investigation on the the effect of As clustering in the dilute-As GaNAs alloy with higher As-content is still required.

IV. Interband Auger Recombination in Dilute-As GaNAs Alloy

The energy band gap coverage presented by dilute-As GaNAs alloy enables the applications for high-power III-Nitride visible LEDs. An important limiting factor for LEDs development is the 'efficiency-droop' issue, which results in significant reduction in internal quantum efficiency in LEDs at high injection current density level. Various theoretical and experimental works had been carried out to elucidate on the physics of the efficiency-droop phenomena in InGaN QW LEDs [4], [33]–[41]. Recently, Delaney and co-workers proposed that the interband Auger recombination contributes considerably to the droop for green-emitting InGaN QWs [33], and the primary factor leading to the interband Auger process can be attributed to the energy difference between the energy gap (E_g) and the Δ interband separation ($\Delta = 1^{st}$ and 2^{nd} conduction band separation) that is within the resonance condition ($|E_g\text{-}\Delta| < 0.15$ eV) for InGaN alloy emitting at green spectral regime [33].

A simple analytical function as a function of the energy separation (E_g-Δ) is introduced in Fig. 7 in order to interpret the data shown in Fig. 8. The Auger function is proportional to the exponential of energy separation (E_g-Δ). The dominant factor determining the Auger coefficient is due to the energy separation (E_g-Δ) [42], and hence the Auger coefficient is proportional to the Auger function model [42]. There are two conditions (a) $E_g > \Delta$ and (b) $E_g < \Delta$ considered in our study.

Under the $E_g > \Delta$ condition, the Auger function is proportional to the exponential term $\exp[-(E_g\text{-}\Delta)/2kT]$. Note that the carrier effective masses are assumed as constant and to possess similar value, resulting in the above simplified expression form. However, under the $E_g < \Delta$ condition, carrier effective masses are excluded from the expression and hence the Auger function is proportional to the exponential term $\exp[-(\Delta\text{-}E_g)/kT]$. In both expressions, the parameter k refers to Boltzmann constant, and the parameter T corresponds to temperature ($T = 300$ K). It is also important to note that the changes in effective mass

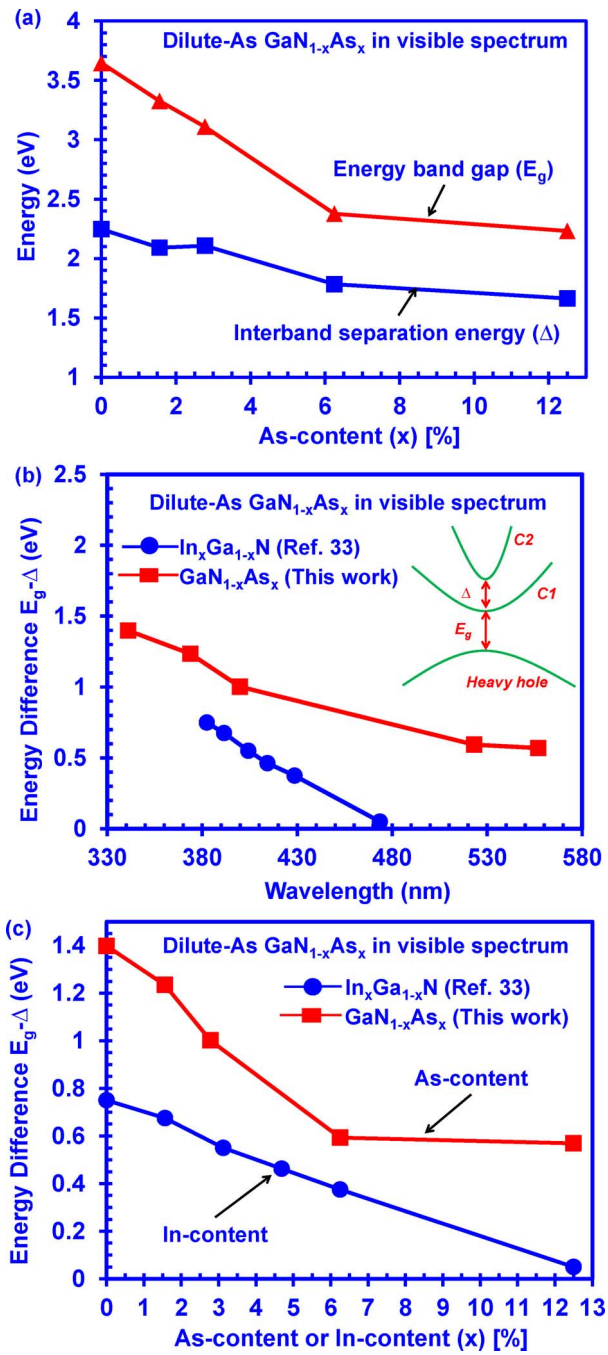

Fig. 8. (a) Comparison between energy band gap E_g and interband separation energy Δ of GaNAs alloy from 0% up to 12.5% As-content and (b) Comparison between the energy difference E_g-Δ of GaNAs alloy and InGaN alloy as a function of emission wavelength/As-content and (c) Comparison of the energy difference E_g-Δ as a function of As-content up to 12.5%.

would have a secondary effect on the Auger function, and consequently the interband Auger recombination rate. For example, as mentioned earlier in the band parameter sections, the significant increases of heavy hole effective masses in low As-content GaNAs alloy would modify the heavy hole band resulting in flatter band profile. Due to the conservation of energy and momentum, it is expected to give rise to a slightly different exponential decaying function in the Auger function, which would then be inflicted onto the interband Auger recombination rate. Nevertheless, the carrier effective masses in this work are assumed to be constant for the sake of simplicity. In our simple model, the physical understanding behind the expression can be interpreted as following. When the energy band gap is smaller than the interband separation energy, the Auger process rate will decrease sharply since the energy conservation needs to be satisfied. When the energy band gap is larger than the interband separation energy, there are some possibilities that an electron would be excited to the second lowest conduction band. Yet, due to the restriction of energy and momentum conservation, the Auger process rate will decrease quickly, in a slower rate compared to the former occasion. In both cases, the given exponential term demonstrates that when the energy band gap is similar to the interband separation energy, on-resonance condition is fulfilled and the Auger process could occur easily. Quasi-resonance and off-resonance conditions are introduced to explain the transition from on-resonant energy to off-resonant energy. When the $|E_g\text{-}\Delta|$ is less than 0.15 eV [33], the f_{Auger} is no longer in the peak region resulting in quasi-resonance condition.

Fig. 8(a) shows the comparison between the energy band gap and the Δ interband separation energy of dilute-As GaNAs alloy from 0% up to 12.5% As-content. Interestingly, the Δ interband separation energy decreases as the As-content increases in the GaNAs alloy while the interband separation energy of the InGaN alloy increases as the In-content increases in the alloy [33]. Fig. 8(b) and (c) presents the energy difference (E_g-Δ) as a function of emission wavelengths and impurity contents for dilute-As GaNAs alloys respectively. From these two figures [Fig. 8(a) and (b)], it is shown that dilute-As GaNAs alloy has emission wavelength up to 525 nm (green) with only 6.25% As-content. The incorporation of In-content up to 12% in InGaN alloy resulted in emission wavelength of ~ 480 nm [33].

The comparisons on the energy differences (E_g-Δ) for the dilute-As GaNAs alloy and InGaN alloy [33] are presented in the Fig. 8(b) and 8(c). The (E_g-Δ) reduces when the As-concentration is gradually increased in the GaNAs alloy. Similar trend is also observed in the InGaN alloy. It is worth to note that although the (E_g-Δ) of dilute-As GaNAs alloy decreases, the (E_g-Δ) for all the investigated GaNAs alloys are larger than 0.57 eV which correspond to off-resonance Auger process. In contrast, the (E_g-Δ) for InGaN alloy [Fig. 8(b) and 8(c)] approaches the resonance condition at $\lambda \sim 480$ nm and In-content of $\sim 12\%$ [33]. This finding strongly indicates that the interband Auger process in dilute-As GaNAs alloy as relatively negligible for serving as active material with emission wavelength in visible spectral regimes, specifically in the green spectral regime.

V. Conclusion

In summary, First Principle calculations were carried out by using LDA approximation to examine the band structure of dilute-As GaNAs material. With As-content ranging from 0% up to 12.5%, the band structures of the GaNAs alloy remain direct band gaps with band gap covering from 3.645 eV down to 2.232 eV. The electronic band structure parameters for dilute-As GaNAs alloy are also extracted and presented in this work, which are applicable for device physics analysis and simulation for device technologies employing this alloy. In addition, the off-resonance condition of GaNAs alloy suggests

the minimal Auger interband recombination in the alloy. Our finding indicates the strong potential of the dilute-As GaNAs alloy for green-emitting III-Nitride LEDs.

ACKNOWLEDGMENT

The authors also acknowledge helpful technical discussion with Dr. H. Schweiger from Material Design.

REFERENCES

[1] S. Nakamura, "The roles of structural imperfections in InGaN-based blue light-emitting diodes and laser diodes," *Science*, vol. 281, no. 5379, pp. 956–961, Aug. 1998.

[2] M. H. Crawford, "LEDs for solid-state lighting: Performance chanllenges and recent advances," *IEEE J. Sel. Topics Quantum Electron.*, vol. 15, no. 4, pp. 1028–1040, Jul./Aug. 2009.

[3] H. Zhao, G. Y. Liu, J. Zhang, J. D. Poplawsky, V. Dierolf, and N. Tansu, "Approaches for high internal quantum efficiency green InGaN light-emitting diodes with large overlap quantum wells," *Opt. Express*, vol. 19, no. S4, pp. A991–A1007, Jul. 2011.

[4] H. Zhao, G. Liu, R. A. Arif, and N. Tansu, "Current injection efficiency quenching leading to efficiency droop in InGaN quantum well light-emitting diodes," *Solid State Electron.*, vol. 54, pp. 1119–1124, Oct. 2010.

[5] X. Li, S. Kim, E. E. Reuter, S. G. Bishop, and J. J. Coleman, "The incorporation of arsenic in GaN by metalorganic chemical vapor deposition," *Appl. Phys. Lett.*, vol. 72, no. 16, pp. 1990–1992, Feb. 1998.

[6] X. Li, S. G. Bishop, and J. J. Coleman, "GaN epitaxial lateral overgrowth and optical characterization," *Appl. Phys. Lett.*, vol. 73, no. 9, pp. 1179–1181, Jul. 1998.

[7] X. Li, H. Liu, X. Ni, U. Ozgur, and H. Morkoc, "Effect of carrier spillover and Auger recombination on the efficiency droop in InGaN-based blue LEDs," *Superlattices and Microstructures*, vol. 47, pp. 118–122, Jan. 2010.

[8] X. H. Li, R. Song, Y. K. Ee, P. Kumnorkaew, J. F. Gilchrist, and N. Tansu, "Light extraction efficiency and radiation patterns of III-nitride light-emitting diodes with colloidal microlens arrays with various aspect ratios," *IEEE Photon. J.*, vol. 3, no. 3, pp. 489–499, Jun. 2011.

[9] I. H. Brown, P. Blood, P. M. Smowton, J. D. Thomson, S. M. Olaizola, A. M. Fox, P. J. Parbrook, and W. W. Chow, "Time evolution of the screening of piezoelectric fields in InGaN quantum wells," *IEEE J. Quantum Electron.*, vol. 42, no. 12, pp. 1202–1208, Nov./Dec. 2006.

[10] N. Tansu, J. Y. Yeh, and L. J. Mawst, "High-performance 1200-nm InGaAs and 1300-nm InGaAsN quantum-well lasers by metalorganic chemical vapor deposition," *IEEE J. Sel. Topics Quantum Electron.*, vol. 9, no. 5, pp. 1220–1227, Sep. 2003.

[11] S. R. Bank, L. L. Goddard, M. A. Wistey, H. B. Yuen, and J. S. Harris, "On the temperature sensitivity of 1.5-μm GaInNAsSb lasers," *IEEE J. Sel. Topics Quantum Electron.*, vol. 11, no. 5, pp. 1089–1098, Sep./Oct. 2005.

[12] A. Lindsay and E. P. O'Reilly, "Unification of the band anticrossing and cluster-state models of dilute nitride semiconductor alloys," *Phys. Rev. Lett.*, vol. 93, p. 196402, Nov. 2004.

[13] K. Uesugi, N. Morooka, and I. Suemune, "Reexamination of N composition dependence of coherently grown GaNAs band gap energy with high-resolution x-ray diffraction mapping measurements," *Appl. Phys. Lett.*, vol. 74, no. 9, pp. 1254–1256, Mar. 1999.

[14] L. Xu, D. Patel, C. S. Menoni, J. Y. Yeh, L. J. Mawst, and N. Tansu, "Optical determination of the electron effective mass of strain compensated In0.4Ga0.6As0.995N0.005/GaAs single quantum well," *Appl. Phys. Lett.*, vol. 89, no. 17, p. 171112, Oct. 2006.

[15] A. Kimura, C. A. Paulson, H. F. Tang, and T. F. Kuech, "Epitaxial $GaN_{1-y}As_y$ layers with high As content grown by metalorganic vapor phase epitaxy and their band gap energy," *Appl. Phys. Lett.*, vol. 84, no. 9, pp. 1489–1491, Mar. 2004.

[16] K. M. Yu, S. V. Novikov, R. Broesler, C. R. Staddon, M. Hawkridge, Z. Liliental-Weber, I. Demchenko, J. D. Denlinger, V. M. Kao, F. Luckert, R. W. Martin, W. Walukiewicz, and C. T. Foxon, "Non-equilibrium GaNAs alloys with band gap ranging from 0.8–3.4 eV," *Physica Status Solidi (c)*, vol. 7, no. 7–8, pp. 1847–1849, May 2010.

[17] X. H. Li, H. Tong, H. P. Zhao, and N. Tansu, "Band structure calculation of dilute-As GaNAs by first principle," in *Proc. SPIE Photonics West 2010, Phys. & Simulation of Optoelectron. Devices XVIII*, Feb. 2010, p. 75970H.

[18] T. Mattila and A. Zunger, "P-P and As-As isovalent impurity pairs in GaN: Interaction of deep t2 levels," *Phys. Rev. B, Condens. Matter*, vol. 59, no. 15, pp. 9943–9953, Apr. 1999.

[19] C. G. Van de Walle, "Arsenic impurities in GaN," *Appl. Phys. Lett.*, vol. 76, no. 8, pp. 1009–1011, Feb. 2000.

[20] K. Laaksonen, H.-P. Komsa, E. Arola, T. T. Rantala, and R. M. Nieminen, "Computational study of $GaAs_{1-x}N_x$ and $GaN_{1-y}As_y$ alloys and arsenic impurities in GaN," *J. Phys.: Condens. Matter*, vol. 18, pp. 10097–10114, Oct. 2006.

[21] R. A. Arif, H. Zhao, and N. Tansu, "Type-II InGaN-GaNAs quantum wells active regions for lasers applications," *Appl. Phys. Lett.*, vol. 92, p. 011104, Jan. 2008.

[22] H. Zhao, R. A. Arif, and N. Tansu, "Self consistent gain analysis of type-II 'W' InGaN-GaNAs quantum well lasers," *J. Appl. Phys.*, vol. 104, p. 043104, Aug. 2008.

[23] J. Wu, W. Walukiewicz, K. M. Yu, J. D. Denlinger, W. Shan, J. W. Ager, III, A. Kimura, H. F. Tang, and T. F. Kuech, "Valence band hybridization in N-rich $GaN_{1-x}As_x$ alloys," *Phys. Rev. B, Condens. Matter*, vol. 70, no. 11, p. 115214, Sep. 2004.

[24] Material Designs Inc., Sante Fe, NM, USA, "MedeA-VASP," [Online]. Available: http://www.materialsdesign.com.

[25] V. Fiorentini and A. Baldereschi, "Dielectric scaling of the self-energy scissor operator in semiconductors and insulators," *Phys. Rev. B, Condens. Matter*, vol. 51, no. 23, pp. 17196–17198, Jun. 1995.

[26] G. Kresse and J. Furthmuller, "Efficient iterative schemes for ab initio total-energy calculations using a plane-wave basis set," *Phys. Rev. B, Condens. Matter*, vol. 54, no. 16, pp. 11169–11186, Oct. 1996.

[27] M. Shishkin, M. Marsman, and G. Kresse, "Accurate quasiparticle spectra from self-consistent GW calculations with vertex corrections," *Phys. Rev. Lett.*, vol. 99, no. 24, p. 246403, Dec. 2007.

[28] P. D. C. King, T. D. Veal, F. Fuchs, Ch. Y. Wang, D. J. Payne, A. Bourlange, H. Zhang, G. R. Bell, V. Cimalla, O. Ambacher, R. G. Egdell, F. Bechstedt, and C. F. McConville, "Band gap, electronic structure, and surface electron accumulation of cubic and rhombohedral In_2O_3," *Phys. Rev. B, Condens. Matter*, vol. 79, no. 20, p. 205211, May 2009.

[29] Y. P. Varshni, "Temperature dependence of the energy gap in semiconductors," *Physica*, vol. 34, no. 1, pp. 149–154, 1967.

[30] I. Vurgaftman, J. R. Meyer, and L. R. Ram-Mohan, "Band parameters for III-V compound semiconductors and their alloys," *J. Appl. Phys.*, vol. 89, no. 11, pp. 5815–5875, Jun. 2001.

[31] M. Suzuki and T. Uenoyama, "First-principles calculations of effective-mass parameters of AlN and GaN," *Phys. Rev. B, Condens. Matter*, vol. 52, no. 11, pp. 8132–8139, Sep. 1995.

[32] S. J. Sweeney, Z. Batool, K. Hild, S. R. Jin, and T. J. C. Hosea, "The potential role of bismide alloys in future photonic devices," in *13th Int. Conf. on Transparent Opt. Networks (ICTON)*, Jun. 2011.

[33] K. T. Delaney, P. Rinke, and C. G. Van de Walle, "Auger recombination rates in nitrides from first principles," *Appl. Phys. Lett.*, vol. 94, no. 19, p. 191109, May 2009.

[34] M. Krames, O.B. Shchekin, R. Mueller-Mach, G.O. Mueller, L. Zhou, G. Harbers, and M.G. Craford, "Status and future of high-power light-emitting diodes for solid-state lighting," *J. Display Technol.*, vol. 3, no. 2, pp. 160–175, Jun. 2007.

[35] J. Hader, J. V. Moloney, B. Pasenow, S. W. Koch, M. Sabathil, N. Linder, and S. Lutgen, "On the importance of radiative and Auger losses in GaN-based quantum wells," *Appl. Phys. Lett.*, vol. 92, no. 26, p. 261103, Jul. 2008.

[36] E. Kioupakis, P. Rinke, K. T. Delaney, and C. G. Van de Walle, "Indirect Auger recombination as a cause of efficiency droop in nitride light emitting diodes," *Appl. Phys. Lett.*, vol. 98, p. 161107, Apr. 2011.

[37] Y. C. Shen, G. O. Mueller, S. Watanabe, N. F. Gardner, A. Munkholm, and M. R. Krames, "Auger recombination in InGaN measured by photoluminescence," *Appl. Phys. Lett.*, vol. 91, p. 141101, Oct. 2007.

[38] M. H. Kim, M. F. Schubert, Q. Dai, J. K. Kim, E. F. Schubert, J. Piprek, and Y. Park, "Origin of efficiency droop in GaN-based light-emitting diodes," *Appl. Phys. Lett.*, vol. 91, p. 183507, Oct. 2007.

[39] S. F. Chichibu, T. Azuhata, M. Sugiyama, T. Kitamura, Y. Ishida, H. Okumura, H. Nakanishi, T. Sota, and T. Mukai, "Optical and structural studies in InGaN quantum well structure laser diodes," *J. Vacuum Sci. Technol. B: Microelectron. and Nanometer Structures*, vol. 19, no. 6, pp. 2177–2183, Nov. 2001.

[40] J. Xie, X. Ni, Q. Fan, R. Shimada, U. Ozgur, and H. Morkoc, "On the efficiency droop in InGaN multiple quantum well blue light emitting diodes and its reduction with p-doped quantum well barriers," *Appl. Phys. Lett.*, vol. 93, no. 12, p. 121107, Sep. 2008.

[41] A. A. Efremov, N. I. Bochkareva, R. I. Gorbunov, D. A. Lavrinovich, Y. T. Rebane, D. V. Tarkhin, and Y. G. Shreter, "Effect of the joule heating on the quantum efficiency and choice of thermal conditions for high-power blue InGaN/GaN LEDs," *Semicond.*, vol. 40, pp. 605–610, May 2006.
[42] A. Sugimura, "Band-to-band Auger effect in long wavelength multinary III-V semiconductor lasers," *IEEE J. Quantum Electron.*, vol. QE-18, no. 3, pp. 352–363, Mar. 1982.

Chee-Keong Tan received the B.S. degree in electrical engineering (First Class Honors) from the University of Sheffield, Sheffield, U.K., in 2011, and since July 2011, he has been a graduate student in the Department of Electrical and Computer Engineering at Lehigh University, Bethlehem, PA, USA.

His research works are in the field of semiconductor optoelectronics, MOCVD epitaxy, and device fabrication of III-Nitride LEDs. His research focus also includes studying the fundamental electronic structures in nitride material and efficiency droop in light emitting diodes.

Jing Zhang received the B.S. degree in electronic science and technology from Huazhong University of Science and Technology, Wuhan, China, in June 2009, and has been working toward the Ph.D. degree in the Department of Electrical and Computer Engineering (ECE) and the Center for Photonics and Nanoelectronics (CPN) at Lehigh University, Bethlehem, PA, USA, since 2009.

Her research areas are related to III-Nitride semiconductor nanostructures for thermoelectric and solid state lighting technologies. Her research works cover various aspects of computational, growths, and device fabrication of III-Nitride semiconductor for photonics and thermoelectric applications. Her research topics include the pursuit of novel materials for high thermoelectric figure of merit, and solid state lighting applications.

Ms. Zhang is a recipient of the Dean's Scholarship from Lehigh University in 2009, Best Graduation Thesis from Huazhong University of Science and Technology in 2009, and the SPIE Scholarship in Optics and Photonics from Lehigh University.

Xiao-Hang Li received the B.S. degree in applied physics from Huazhong University of Science and Technology, Wuhan, China, in 2008, the M.S. degree from Lehigh University, Bethlehem, PA, USA, in May 2011, and is currently pursuing the Ph.D. degree from the Department of Electrical and Computer Engineering (ECE) at Georgia Institute of Technology, Atlanta, GA, USA.

While working towards the M.S. degree, he was a Research Assistant in ECE and the Center for Photonics and Nanoelectronics at Lehigh University from July 2008 to May 2011. His research interests are related to III-Nitride semiconductor based material growth and optoelectronic devices, including MOCVD, device fabrication and characterization for III-Nitride light-emitting diodes (LEDs), and laser diodes (LD) from deep UV to green spectra.

Guangyu Liu received the B.S. degree in electronic science and technology from Huazhong University of Science and Technology, Wuhan, China, in June 2008, and has been working toward the Ph.D. degree in the Department of Electrical and Computer Engineering (ECE) and the Center for Photonics and Nanoelectronics at Lehigh University, Bethlehem, PA, USA, since July 2008.

Her research interests are related to III-Nitride semiconductor nanostructures and optoelectronics devices, covering the theoretical/computational, metalorganic chemical vapor deposition (MOCVD) growth, and device fabrication and characterization technology. The research topics include the pursuit of high-performance III-Nitride light-emitting diodes (LEDs), the growths of III-Nitride quantum dots (QDs) devices for solid state lighting and solar cells, and investigation of III-Nitride-based intersubband quantum cascade laser (QCL).

Ms. Liu has published more than 50 refereed journal and conference publications. She is also a recipient of the SPIE Scholarship in Optics and Photonics from Lehigh University, the Sherman-Fairchild Fellowship from Lehigh University, the Dean's Scholarship from Lehigh University, and Best Graduation Thesis from Huazhong University of Science and Technology.

Benjamin O. Tayo received the B.Sc. (Hons.) in physics and computer science from University of Buea, Buea, Cameroon, in 2004, the M.Sc. degree (with distinction) in theoretical condensed matter physics from the University of Trieste, Trieste, Italy, in 2007, and received the Ph.D. degree in physics Lehigh University, Bethlehem, PA, USA, in 2012.

In fall of 2007, he became a Graduate Teaching/Research Assistant at Lehigh University. Since fall 2012, he has been a Postdoctoral Research Fellow/Research Scientist in the MOCVD and Nanophotonics Lab (Tansu Group) at Lehigh University, Bethlehem, PA, USA. His current research interests involve theoretical/computational aspects of the physics of III-Nitride materials, Auger recombination theory in nitride materials, and various aspects of the physics of carbon-based materials for novel applications in optoelectronics.

Dr. Tayo was awarded the prestigious Abdus Salam International Center for Theoretical Physics-University of Trieste Joint Scholarship for higher education in physics after a one-year postgraduate study in physics at University of Buea.

Nelson Tansu was born in 1977. He received the B.S. degree in applied mathematics, electrical engineering, and physics (with Highest Distinction) and the Ph.D. degree in electrical engineering/applied physics from the University of Wisconsin-Madison, Madison, WI, USA, in 1998 and 2003, respectively.

Since July 2003, he has been a faculty member in the Department of Electrical and Computer Engineering (ECE) and Center for Photonics and Nanoelectronics (CPN) at Lehigh University, Bethlehem, PA, USA, where he currently is the Class of 1961 Associate Professor (with tenure). He currently serves as Associate Editor for *OSA Optical Materials Express* (2010–present), Assistant/Associate Editor for *Nanoscale Research Letters* (2007–present), and Editor-in-Chief for *Optics* (2013–present). He has published in over 240 refereed international journals (92) and conference (150+) publications, and holds several U.S. patents (total > 10). He also regularly reviews leading journals in applied physics, quantum electronics, nanotechnology, photonics, and optoelectronics areas. Previously, he has given numerous lectures, seminars, and keynote and invited talks (total > 45) at universities, research institutions, and conferences in the Canada, Europe, and Asia. His research works cover both the theoretical and experimental aspects of the physics of semiconductor optoelectronics materials and devices, the physics of low-dimensional semiconductor (nanostructure), and MOCVD and device fabrications of III-Nitride and III-V-Nitride semiconductor optoelectronics devices on GaAs, InP, and GaN substrates.

Dr. Tansu served as the Primary Guest Editor of the IEEE JOURNAL OF SELECTED TOPICS IN QUANTUM ELECTRONICS (2008–2009) and IEEE/OSA JOURNAL OF DISPLAY TECHNOLOGY (2012–2013), and he also serves as an Associate Editor for IEEE PHOTONICS JOURNAL (2009–present). He served on the Technical Program Committee for several major technical conferences for IEEE, OSA, SPIE, and APS, including IEEE/OSA Conference on Lasers and Electro-Optics (2007–2009, 2013), SPIE Photonics West (2009–2013), APS March Annual Meeting (2007, 2009–2011), and ACP (2012, 2013), and others. He was selected as Invited General Participant at the 2008 National Academy of Engineering (NAE)'s U.S. Frontiers of Engineering (FOE) Symposium, and he served as the Organizing Committee for the 2009 NAE's U.S. Frontiers of Engineering Symposium. Recently, he has been invited to participate in the NAE's 2012 German-American Frontiers of Engineering Symposium (GAFOE).